# Confidence and efficiency scaling in Variational Quantum Monte Carlo calculations

F. Delyon,[1] B. Bernu,[1] and Markus Holzmann[2]

[1] *LPTMC, UMR 7600 of CNRS, Université P. et M. Curie, Paris, France*
[2] *LPMMC, UMR 5493 of CNRS, Université Grenoble Alpes, B.P. 166, 38042 Grenoble, France*

(Dated: September 12, 2016)

Based on the central limit theorem, we discuss the problem of evaluation of the statistical error of Monte Carlo calculations using a time discretized diffusion process. We present a robust and practical method to determine the effective variance of general observables and show how to verify the equilibrium hypothesis by the Kolmogorov-Smirnov test. We then derive scaling laws of the efficiency illustrated by Variational Monte Carlo calculations on the two dimensional electron gas.

PACS numbers: 02.50.Ey, 02.70.Ss, 02.70.Rr, 02.70.Tt, 71.10.Ca

arXiv:1609.02703v1 [physics.comp-ph] 9 Sep 2016

## I. INTRODUCTION

Monte Carlo integration techniques have become a standard tool in statistical physics and classical and quantum many body theory[1,4]. However, due to the finite simulation time, outcomes of such calculations are affected by statistical uncertainties and the precise estimation of the resulting error is essential to obtain quantitative results.

Standard Monte Carlo methods are based on Markov diffusion processes using Metropolis-Hastings algorithm. There, sequential outputs are not independent, and, similar to any other statistical method, the main problem is to estimate the robustness of the sampling.

As one usually deals with a very large configuration space, an exact answer is impossible. Modestly, one expects that a finite number of samples may reflect the expectation on the whole space, and we want to ensure the coherence of our statistics. That is, we want to check the stationarity of our sampling and to estimate the accuracy of some averaged quantity.

The aim of this work is to show that the central limit theorem (CLT) and the Kolmogorov-Smirnov theorem provide simple tools to determine the accuracy of some observable and to test the coherence of the sampling. These well known tools have already been discussed in this context[1–3], here we provide an effective implementation of these mathematical results.

In the following, most examples come from Variational Quantum Monte-Carlo (VMC) calculations applied to the 2D homogeneous electron gas in a quadratic box of length $L$ with periodic boundary conditions[5]. The configuration space is $[-L/2, L/2]^\nu$ where $\nu = 2N_e$ for the $N_e$ electrons, and we define the dimensionless parameter $r_s$ by $\pi a_B^2 r_s^2 N_e = L^2$ where $a_B$ is the Bohr radius.

Given a complex antisymmetric function $\Psi(r_1, \ldots, r_{N_e})$ of the Slater-Jastrow form, we concentrate on one of the most important quantity, the average energy, $\mathcal{E}$, of this state:

$$\mathcal{E} = \frac{\langle \Psi | H | \Psi \rangle}{\langle \Psi | \Psi \rangle} \tag{1}$$

where $H$ is the electronic Hamiltonian.

In fact the above integration is rapidly unfeasible as the number of electrons increases. In Sect.II we briefly explain the standard VMC approach to compute the above integral for large values of $N_e$. Our estimation of the statistical error relies on the CLT is described and tested in Sect.III. In Sect. IV, we show how the Kolmogorov-Smirnov test can be implement to decide on the consistency of the statistical distributions. The efficiency and optimal behavior of VMC with respect to the size $N_e$ and the discretization of the Markov process is discussed in Sect.V.

## II. DISCRETIZED DIFFUSION ALGORITHM

We start with a brief description of the standard algorithm used for Variational Monte Carlo calculations.

Let $P(R)dR$ be a probability on $\mathbb{R}^\nu$, the idea of Monte Carlo methods[4] is to calculate expectations using a multidimensional diffusion process. Indeed, if $R(t)$ is an ergodic Markov process with invariant measure $P(R)dR$ then:

$$\lim_{T\to\infty} \frac{1}{T} \int_0^T f(R(t))dt = \int f(R)P(R)dR \tag{2}$$

provided that $\int |f(R)|P(R)dR < +\infty$.

Thus, one has to choose a diffusion process such that the invariant distribution is exactly $P$. Let $R(t)$ be given by the Langevin equation[6]:

$$dR(t) = G(R)dt + dw \tag{3}$$

$w$ is a vector of $\nu$ independent Brownian motions (Wiener processes) and $G$ a vector of $\nu$ regular functions.

The corresponding Kolmogorov[7] (or Fokker-Planck) forward equation for a measure $\mu(R,t)dR$ is:

$$\frac{\partial \mu}{\partial t} = -\nabla G\mu + \frac{1}{2}\Delta\mu \tag{4}$$

and choosing

$$G = \frac{1}{2}\nabla \ln(P) \tag{5}$$

$P(R)dR$ is an invariant measure of Eq. (4).

For numerical simulations, one approximates the process, Eq. (3), with the following discrete process:

$$R_{i+1} = R_i + G(R_i)\tau + w(\tau) \tag{6}$$

As $\tau$ goes to zero we expect that the invariant probability of Eq. (6) goes to $P$. The integral kernel of the Markov process (6) is:

$$T(R'|R) = \frac{1}{(2\pi\tau)^{\nu/2}} \exp(-\frac{(R' - R - G(R)\tau)^2}{2\tau}) \tag{7}$$

In practice, to avoid convergence analysis, one uses the Metropolis[8] algorithm to obtain precisely $P$ as the invariant measure. First, starting at $R$, we choose the next point $R'$ according to Eq. ( 7). Thereafter, we use an auxiliary boolean independent variable in order to accept or reject the new point with probability $A(R', R)$ such that $P$ is invariant. Equivalently, we have to choose $A(R', R)$ such that the mean value of any function $f(R)$ is invariant

$$\int f(R)P(R)dR = \int f(R')A(R', R)T(R'|R)P(R)dRdR' + \int f(R)P(R)\left[1 - \int A(R', R)T(R'|R)dR'\right]dR$$

i.e.

$$\int dR'\, T(R|R')A(R, R')P(R') = \int dR'\, T(R'|R)A(R', R)P(R). \tag{8}$$

This condition is fulfilled imposing detailed balance:

$$T(R|R')A(R, R')P(R') = T(R'|R)A(R', R)P(R). \tag{9}$$

Hence, the optimal (minimal rejection) solution is given by

$$A(R', R) = \min\left(1, \frac{T(R|R')P(R')}{T(R'|R)P(R)}\right). \tag{10}$$

If we reject the new point, the point $R$ is counted twice. Starting from $R_1$ and iterating this process, we obtain a sequence of vectors $(R_1, R_2, \dots)$ and a sequence of integral weights $(n_1, n_2, \dots)$ where $n_i$ is the number of repetitions of the vector $R_i$. This sequence asymptotically reflect the distribution $P$.

The acceptance rate $\mathsf{R}_a$, is the probability that a move is accepted, thus

$$\mathsf{R}_a = \frac{\sum 1}{\sum n_i} \to \frac{1}{E(n)} \tag{11}$$

where $E(.)$ stands for the expectation of a random variable.

For a function $X(R)$, we associate the process $(X_i = X(R_i))$, and the empirical expectation of the variable $X$ is given by:

$$\overline{X}_N = \frac{\sum_{i=1}^N X_i n_i}{\sum_{i=1}^N n_i} \tag{12}$$

The main problem is to estimate the robustness of a sampling $\{X_i, n_i\}$.

In our case, $\nu = 2N_e$ and $R$ is sampled with a probability proportional to $|\Psi(R)|^2 dR$; that is $G(R) = \nabla \ln |\Psi(R)|$.

Setting

$$X_i(R_i) = \frac{(H\Psi)(R_i)}{\Psi(R_i)} \tag{13}$$

we expect for a fair sampling of the total energy

$$\frac{\sum_i X_i n_i}{\sum_i n_i} \to \frac{\int (H\Psi)(R)\overline{\Psi}(R)dR}{\int |\Psi(R)|^2 dR} = \frac{\langle\Psi|H|\Psi\rangle}{\langle\Psi|\Psi\rangle} \tag{14}$$

## III. THE CENTRAL LIMIT THEOREM

The central limit theorem(CLT) is a well-known result for independent identically distributed random variables providing the expected fluctuations of the mean of a random sequence. This theorem has many generalizations in particular for Markov process[9–12].

Let $(Y_1, Y_2, \dots)$ be a stationary mixing Markov process with invariant probability $\pi$ and $E(|Y|) < +\infty$. Let

$$\tilde{Y}_i = Y_i - E(Y) \tag{15}$$

and $\mathcal{N}(a, \sigma^2)$ be the Gaussian law of mean $a$ and variance $\sigma^2$, then the ergodic theorem guarantees that

$$Z_N = \frac{1}{\sqrt{N}} \sum_{i=1}^N \tilde{Y}_i \tag{16}$$

goes to zero with probability one. A central limit theorem (CLT) for Markov process gives conditions under which

$$Z_N \xrightarrow{\mathcal{D}} \mathcal{N}(0, \sigma^2_{\text{eff}}) \tag{17}$$

where

$$\sigma^2_{\text{eff}} = E(\tilde{Y}_1^2) + 2\sum_{k>1} E(\tilde{Y}_1 \tilde{Y}_k). \tag{18}$$

and $\mathcal{D}$ stands for the convergence in distribution. Equation (18) can be easily guessed since $\sigma^2_{\text{eff}}$ corresponds to the limit of $E\left(Z_N^2\right)$ as soon as

$$C_k = E(\tilde{Y}_1 \tilde{Y}_{k+1}) \tag{19}$$

decreases rapidly as $k$ increases. Here we suppose that this is our case and that the CLT is in force; the problem is how to estimate $\sigma_{\text{eff}}$ for finite samplings.

### A. Determination of the effective variance

For an empirical sampling $(Y_i)_{i=1}^N$, the empirical estimate for $E(Y)$ is

$$\overline{Y}_N = \frac{1}{N}\sum_{i=1}^{N} Y_i \tag{20}$$

and if we define

$$C_{N,k} = \frac{1}{N}\sum_{i=1}^{N-k}(Y_i - \overline{Y}_N)(Y_{i+k} - \overline{Y}_N) \tag{21}$$

we have $\lim_{N\to\infty} C_{N,k} = C_k$. We then have

$$\sigma^2_{\text{eff}} = \lim_{N\to\infty} C_{N,0} + 2\lim_{n\to\infty}\sum_{k=1}^{n}\lim_{N\to\infty} C_{N,k} \tag{22}$$

Notice that the order of the two limits is important, as we also have

$$\begin{aligned} C_{N,0} + 2\sum_k C_{N,k} &= \frac{1}{N}\sum_{i,j}(Y_i - \overline{Y}_N)(Y_j - \overline{Y}_N) \\ &= 0 \end{aligned} \tag{23}$$

In order to impose the right order of the limit, we use a so-called window estimator[10] in the following

$$\sigma^2_{\text{eff}}(k) = C_{N,0} + 2\sum_{i=1}^{k} C_{N,i} \tag{24}$$

with $1 \ll k \ll N$. The main difficulty is the choice of $k$ such that $\sigma^2_{\text{eff}}(k_l)$ provides a robust estimate for the true uncertainty: too small values of $k$ may considerably underestimate the error, whereas large values of $k_m$ will mainly add noise such that $\sigma^2_{\text{eff}}(k)$ becomes unreliable.

Indeed, even if we assume that $C_k$ decreases quickly, for large $k$, $C_{N,k}$ is a random variable of order $1/\sqrt{N}$. From

$$\begin{aligned} C_{N,k} =& \frac{1}{N}\sum_{i=1}^{N-k}(\tilde{Y}_i + E(Y) - \overline{Y}_N)(\tilde{Y}_{i+k} + E(Y) - \overline{Y}_N) \\ =& \frac{1}{N}\sum_{i=1}^{N-k}\tilde{Y}_i\tilde{Y}_{k+i} - (E(Y) - \overline{Y}_N)^2 \\ & - \frac{1}{N}\left(\sum_{i=1}^{k-1}\tilde{Y}_i + \sum_{i=N-k}^{N}\tilde{Y}_i\right)(E(Y) - \overline{Y}_N) \qquad (25) \\ =& \left(\frac{1}{N}\sum_i \tilde{Y}_i\tilde{Y}_{k+i}\right) - O(1/N), \qquad (26) \end{aligned}$$

we get

$$NC^2_{N,k} = \frac{1}{N}\sum_{i,j}\tilde{Y}_i\tilde{Y}_{k+i}\tilde{Y}_j\tilde{Y}_{k+j} - C_k O(1). \tag{27}$$

and since $C_k$ is assumed to vanish, we get

$$E(NC^2_{N,k}) \to E(Y_0^2) + 2\sum_{j=1}^{+\infty} E(\tilde{Y}_0\tilde{Y}_k\tilde{Y}_j\tilde{Y}_{k+j}). \tag{28}$$

For large $k$, $\tilde{Y}_0$ (resp. $\tilde{Y}_j$) and $\tilde{Y}_k$ (resp.$\tilde{Y}_{k+j}$) are centered independent variables, therefore the non-zero terms in Eq. (28) are for small $j$, and evaluate as:

$$E(\tilde{Y}_0\tilde{Y}_k\tilde{Y}_j\tilde{Y}_{k+j}) \xrightarrow{k\to\infty} E(\tilde{Y}_0\tilde{Y}_j)E(\tilde{Y}_k\tilde{Y}_{k+j}) = C_j^2 \tag{29}$$

Therefore, Eq. (28) asymptotically becomes

$$\Sigma^2 = \lim_{k\to\infty}\lim_{N\to\infty} NE(C^2_{N,k}) = C_0^2 + 2\sum_{j=1}^{+\infty} C_j^2 \tag{30}$$

leading to fluctuations of order $N^{-1/2}$ for $C_{N,k}$ at large $k$.

**Empirical estimation of** $\sigma_{\text{eff}}$, Eq. (22). Let us set:

$$\Sigma^2_{N,k} = C^2_{N,0} + 2\sum_{j=1}^{k} C^2_{N,j}. \tag{31}$$

$\Sigma^2_{N,k}$ is an increasing function of $k$ and for large $k$ it goes like $\Sigma^2(1 + k/N)$. On the other hand $C^2_{N,k}$ is of order one for small $k$ then decreases and oscillates around $\Sigma^2/N$. Thus there is a marginal value $k_m$ corresponding to the first $k$ such that $NC^2_{N,k} < \Sigma^2_{N,k}$ providing a good estimate of the effective variance, Eq. (22). Clearly, this estimate makes sense only if $\sqrt{N}C_{N,k_m} \ll C_0$, otherwise we must consider that $N$ is not large enough.

In the following subsections, we demonstrate the robustness of our error estimation and test its validity against independent data sets.

### B. CLT and Monte Carlo

We can extend the CLT to Monte-Carlo observables considering the weight $n_i$ of the Metropolis part (see section II). Now $\overline{X}_N$ is given by Eq. (12) and setting $\tilde{X}_i = X_i - E(X)$

$$N\left(\frac{\sum \tilde{X}_i n_i}{\sum n_i}\right)^2 \to C_{N,0} + 2\sum_k C_{N,k} \tag{32}$$

where:

$$C_{N,k} = \frac{1}{E(n)(\sum_i n_i)}\sum_{i=1}^{N-k} n_i\tilde{X}_i n_{i+k}\tilde{X}_{i+k} \tag{33}$$

and Eq. (30) is still in force.

Fig. 1 shows a representative example of the behavior of $C_{N,k}$ for a MC simulation with an acceptance rate $\mathsf{R}_a$ of 0.45.

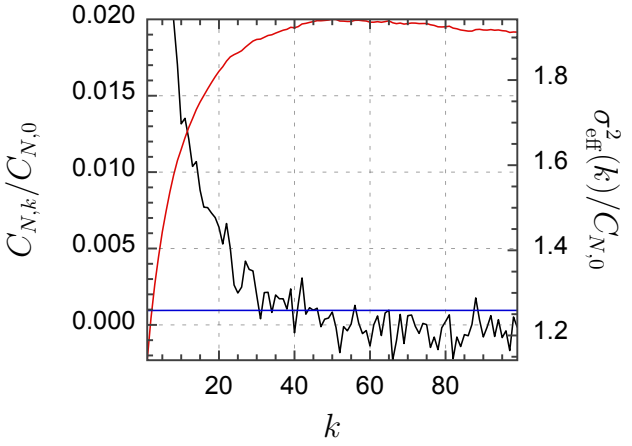


FIG. 1. $C_{N,k}/C_{N,0}$ as a function of $k$ (black line) and $\sigma^2_{\rm eff}(k)/C_{N,0}$ (red line). The blue line is $\Sigma_{N,k}/(\sqrt{N}C_{N,0})$; The crossing of the black and blue curves occurs for $k = 31$ giving $\sigma^2_{\rm eff} = 1.90\ C_0$.

Furthermore, Eq. (29) may be extended to estimate the correlations of $C_{N,k}$:

$$E(NC_{N,k'}C_{N,k+k'}) \xrightarrow{k'\to\infty} \sum_{i=-\infty}^{\infty} C_i C_{i+k} \qquad (34)$$

This shows that $C_{N,k}$ may be strongly correlated. Looking at the red curve of Fig. 1, the cutoff at $k = 31$ may seem unjustified, but different samplings lead to different behavior after this cutoff while the behavior for smaller values of $k$ is robust (Fig. 2).

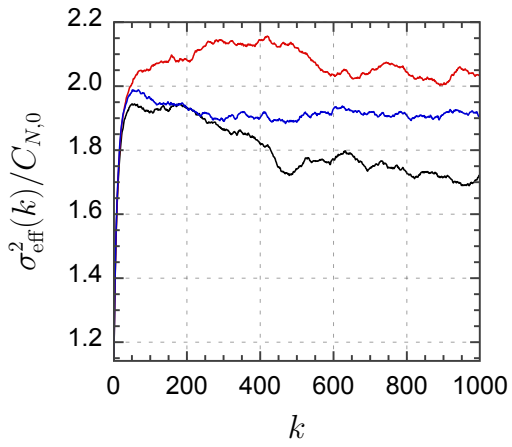


FIG. 2. $\sigma^2_{\rm eff}(k)/C_0$ for three independent samplings.

### C. Comparison with sample fluctuations

We can compare our estimate of the empirical variance with the variance obtained with independent samples. We make $p = 40$ independent samples of $N$=45000 trials.

For each sample $\alpha$ we compute the mean:

$$\overline{X}_\alpha = \frac{\sum_{i=1}^N X_{\alpha,i} n_{\alpha,i}}{\sum_{i=1}^N n_{\alpha,i}} \qquad (35)$$

and we get the empirical mean:

$$\overline{X} = \frac{1}{p}\sum_{\alpha=1}^{p} \overline{X}_\alpha \qquad (36)$$

The variance of $X$ (corresponding to $C_{N,0}$ in Eq. (33)) is 0.308 and taking into account the correlations, Eq. (18), we get $\sigma^2_{\rm eff}$ is 0.591. This gives a standard deviation $\frac{\sigma_{\rm eff}}{\sqrt{N}}$=0.00363 for the $X_\alpha$'s to be compared with 0.00370 obtained directly from the variance of the 40 values of $\overline{X}_\alpha$.

Now we can go further and check the asymptotic normal law of the $X_\alpha$'s. In Fig. 3, we plot the distribution of:

$$x_\alpha = \sqrt{N}\frac{\overline{X}_\alpha - \overline{X}}{\sigma_{\rm eff}}. \qquad (37)$$

supposed to be a normalized centered Gaussian variable. The black curve is the distribution function of a normalized Gaussian. Since the $\overline{X}_\alpha$ are independent, we have:

$$M_{\alpha\beta} = E(x_\alpha x_\beta) \xrightarrow[N\to\infty]{} -\frac{1}{p} + \delta_{\alpha\beta} \qquad (38)$$

The correlation matrix $M$ has eigenvalues 0 (multiplicity 1) and 1 (multiplicity $p-1$). Thus for large $N$, the law of random variable $S = \sum_{\alpha=1}^p x_\alpha^2$ is exactly the law of the sum of the square of $p-1$ normalized Gaussian variables. Therefore, we can use the $\chi^2$ test:

$$P(S < x) = \chi^2_{p-1}(x) = \Gamma\left(\frac{p-1}{2}, \frac{x}{2}\right) \qquad (39)$$

where $\Gamma$ is the regularized incomplete gamma function. Here we have $S = 40.1$ and the $\chi^2_{39}(40.1) = 0.62$.

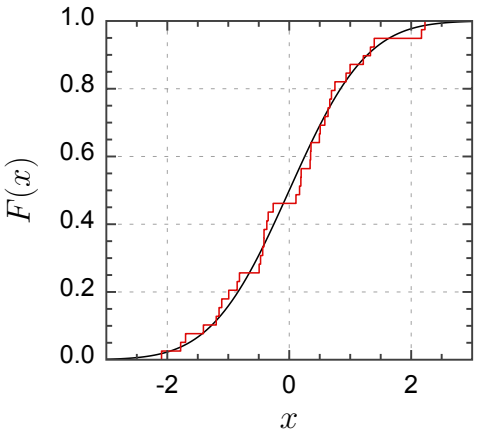


FIG. 3. Distributions of $x = \frac{\overline{X}_\alpha - \overline{X}}{\sigma_{\rm eff}}$ for 40 independent samples of 45000 trials. The black line is the distribution function of the normalized Gaussian.

As the acceptance rate $\mathsf{R}_a$ approaches 1, the dynamic is very slow and the correlations are very important leading to large fluctuations. The following sampling is made of 48 samples of 19000 records. The acceptance rate $\mathsf{R}_a$ is 0.94. In Fig. 4 the scaled correlations $C_k$ are relevant until $k = 3244$ leading to $\sum_{k>0} C_k = 530 C_0$. Thus $\sigma^2_{\text{eff}}$ is about 1060 times larger than $C_0$ leading to an accuracy of 0.00724. This increase of the fluctuations is well verified by the distribution on the 48 means giving an accuracy of 0.00728. The $\chi^2$ test gives 0.53.

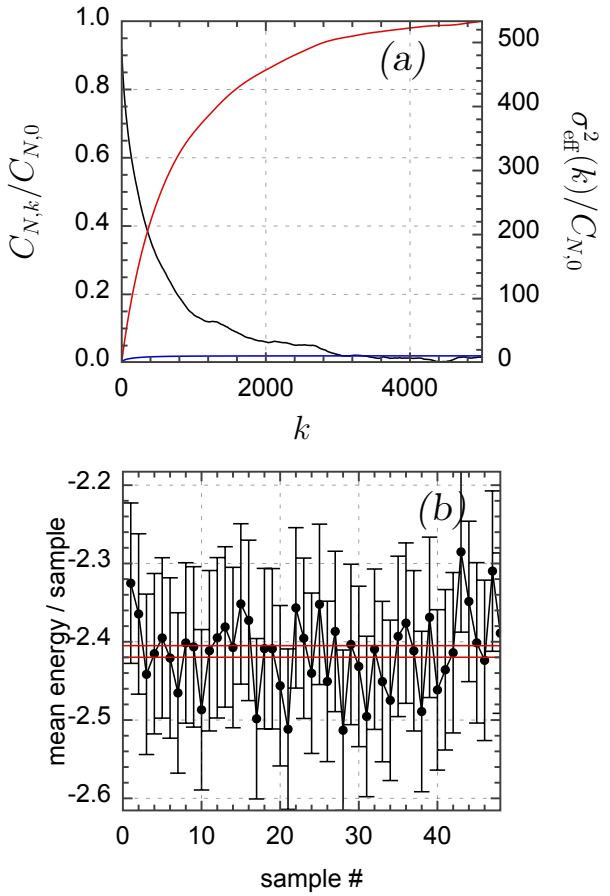


FIG. 4. Example of long correlated walks ($\mathsf{R}_a = 0.94$). (a) Correlations (black line) and running sum of correlations (red line). The blue line is $\Sigma_{N,k}/(\sqrt{N} C_{N,0})$, Eq. (31). (b) mean energy for the 48 samples (arbitrary units).

However, in this case $\sigma^2_{\text{eff}}$ is computed with the 48 samples leading to a marginal $k_m$ such that $C_{k_m}/C_0 \approx 0.02$. The estimate for only one sample gives 0.2 which cannot be consider as small. Thus the 48 samples are relevant for the CLT while a single sample cannot provide any estimate of the accuracy.

## IV. THE KOLMOGOROV-SMIRNOV TEST

Here, we want to provide a quantitative test, based on the Kolmogorov-Smirnov theorem, to verify if the samplings are actually consistent with an equilibrium hypothesis.

### A. The Kolmogorov-Smirnov theorem

First, we briefly recall here the definition and the theorem[6,7]. Let $(Y_1, Y_2, \ldots)$ be independent, identically distributed random variables with continuous distribution function $F$. Let $F_N(x)$ be the empirical distribution function of $(Y_1, Y_2, \ldots Y_N)$:

$$F_N(x) = \frac{1}{N} \sum_i \chi(Y_i < x) \tag{40}$$

where $\chi(b) = 1$ if $b$ is true otherwise 0. As $N$ goes to infinity, by the law of large numbers, $F_N(x) \to F(x)$ almost surely. From the definition:

$$\Delta_N(x) = \sqrt{N}(F_N(x) - F(x)), \tag{41}$$

we have $E(\Delta_N(x)) = 0$ and a straightforward calculation gives for $x \leq y$:

$$E(\Delta_N(x)\Delta_N(y)) = F(x)(1 - F(y)) \tag{42}$$

Thus the CLT for independent variables guarantees

$$\Delta_N(x) \xrightarrow{\mathcal{D}} \mathcal{N}(0, F(x)(1 - F(x))) \tag{43}$$

Let $B(t)$ be the normalized Brownian bridge: the law of Brownian bridge is law of a Brownian motion $b(t)$ such that $b(1) = 0$ (equivalently the law of Brownian bridge $B(t)$ is the law of $b(t) - tb(1)$). For $t \leq t'$

$$E(B(t)B(t')) = t(1 - t') \tag{44}$$

thus $E(\Delta_N(x)\Delta_N(y))$ is exactly the correlation of the Brownian bridge $E(B(t)B(t'))$ at times $t = F(x)$ and $t' = F(y)$.

More precisely, the Kolmogorov-Smirnov theorem tells that

$$D_N = \max_x |\Delta_N(x)| \xrightarrow{\mathcal{D}} D = \max_{0 \leq t \leq 1} |B(t)|. \tag{45}$$

The important point is that the law of $D$ does not depend on the distribution $F$ providing the non-parametric K-S test[13]. The Kolmogorov-Smirnov test evaluates the probability $P(D > D_N)$. The law of $D$ is given by:

$$P(D < x) = 1 + 2 \sum_{n \geq 1} (-1)^n e^{-2n^2 x^2} \tag{46}$$

$$= \frac{\sqrt{2\pi}}{x} \sum_{n \geq 0} e^{-(2n+1)^2 \pi^2/(8x^2)} \tag{47}$$

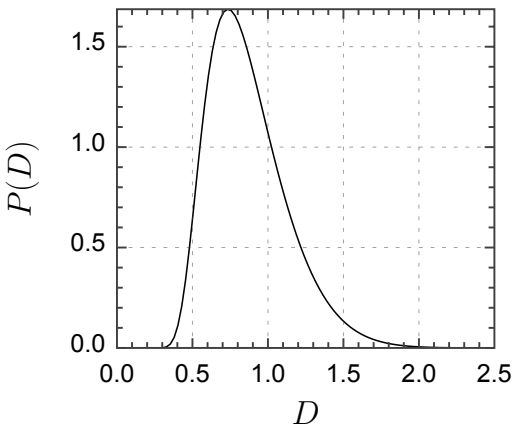


FIG. 5. Density of $D = \max_{0\le t\le 1} |B(t)|$

The density of the probability of $D$ is given on Fig. 5 and for instance $P(D > 2) \approx 7.\,10^{-4}$ and $P(D < 0.3) \approx 9.\,10^{-6}$.

This is the viewpoint of statistics as you need to choose the best candidate among a family of known distribution functions $F_\lambda$. Let us now consider the case where the distribution $F(y)$ in unknown.

### B. Implementation for unknown distribution.

A simple approach is to divide your sample into $p$ samples $\{Y_\alpha\}_{\alpha=1\dots p}$ of length $N$. In order to check homogeneity of the sampling, we first build the distribution $\hat{F}(y)$ of all the samplings. Thereafter, for each samples $Y_\alpha$ we build the distribution function $F_\alpha(y)$ and the differences

$$\Delta_\alpha(y) = \sqrt{N}(F_\alpha(y) - \hat{F}(y)). \tag{48}$$

One checks that for $x < y$:

$$E(\Delta_\alpha(x)\Delta_\beta(y)) = M_{\alpha\beta}F(x)(1 - F(y)) \tag{49}$$

$$M_{\alpha\beta} = \delta_{\alpha\beta} - \frac{1}{p} \tag{50}$$

Thus the $p$ processes are not rigorously independent. As above, the correlation matrix $M$ has $p - 1$ eigenvalues equal to 1 and a null eigenvalue corresponding to the vector $(1, 1, \dots, 1)$. Thus, they represent $p - 1$ independent Brownian bridges and the distribution of $D_\alpha = \max_y \Delta_\alpha(y)$ must be close to distribution of $D$.

On Fig. 6, we compare the statistics obtained with the uniform law on $[0, 1]$: $F(y) = y$. We build a sequence of 30000 independent values. Then we divide the sequence into 30 blocks. The first plot illustrates the difference between $\Delta_1^0(y) = \sqrt{N}(F_1(y) - y)$ and $\Delta_1(y) = \sqrt{N}(F_1(y) - \hat{F}(y))$. The second plot shows the distribution of $D_\alpha^0 = \max_y \Delta_1^0(y)$ and $D_\alpha$.

In turn, the $D_\alpha$'s can be tested against the distribution of maximum of the normalized Brownian bridge. We

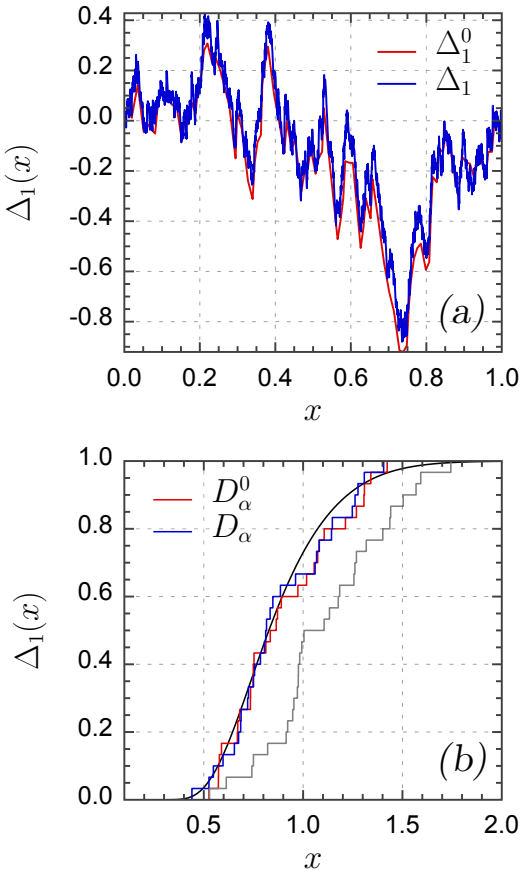


FIG. 6. (a) Comparison of $\Delta_1^0$ and $\Delta_1$. (b) Distributions of $D$ for 30 independent samples of 1000 iid uniform variables; the black line is the distribution of Brownian bridge, Eq. (46). The grey line is obtained by adding a small bias to the sampling.

obtain $D = 0.688$ and $D^0 = 0.664$ corresponding to probabilities $P(D > 0.688) = 0.73$ and $P(D > 0.664) = 0.77$ (probabilities between 0.1 and 0.9 are satisfying, probabilities close to one indicate not independent sampling).

By contrast, the grey curve in Fig. 6(b), is obtained by testing a sample of uniform variables on the interval $[0, 1.02]$ against the uniform law on $[0, 1]$. In this case we obtain $D^0 = 2.59$ corresponding to a probability of $3.0\,10^{-6}$. For the same sampling, the test with the first 10 blocks gives respectively $P = 0.044$ and with 100 blocks of length 1000 we obtain $P = 2.7\,10^{-87}$.

If the variables are not independent, but not strongly correlated, one can apply the Kolmogorov-Smirnov theorem to a subsequence $Y_i^* = Y_{ki}$ where $k$ is of order of the correlation length.

### C. Kolmogorov-Smirnov test for Monte Carlo observables

In our case, the Kolmogorov-Smirnov theorem cannot apply to the process $\{X_i, n_i\}$ whose distribution function is :

$$F_N(x) = \frac{\sum_i \chi(X_i < x) n_i}{\sum_i n_i}. \tag{51}$$

The equivalent of Eq. (42) involves the second moments $E(\chi(X_i < x) n_i^2)$ which cannot be expressed in term of $F(x)$.

Nevertheless, we can check the law of $X_i$ forgetting the weights $n_i$. Instead of the definition Eq. (51), we use:

$$G_N(x) = \frac{1}{N} \sum_i \chi(X_i < x). \tag{52}$$

As above, we have $p$ samples of length $N$ obtained by $p$ equivalent QMC runs. For each sample we compute the distribution function $G_\alpha(y)$ and the distribution $\hat{G}(y)$ for the union of the samples, Eq. (51). Then we set:

$$D_\alpha = \sqrt{N} \sup_y \left| G_\alpha(y) - \hat{G}(y) \right|, \tag{53}$$

Thus, for independent variables, $D_\alpha$ has the law of the maximum absolute value of the Brownian bridge. Fig. 7 shows the distribution of $D_\alpha$ (red curve). The black curve represents the Brownian bridge. We have 40 samples of about 20000 trials.

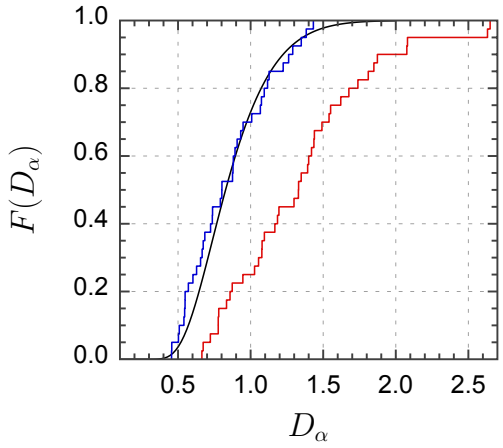


FIG. 7. Distribution functions of $D_\alpha$. The red curve stands for the original sampling. The blue curve is obtained with a stride of 15.

The KS test gives a probability of $7.9\,10^{-10}$ confirming that our samples do not correspond to a sampling of independent variables. The blue curve is obtained with smaller samples retaining one trial for 15 original trials. Indeed, we have $C_{15}/C_0 = 0.01$ while $C_1/C_0 = 0.3$, see Eq. (19). The probability given by the KS test is 0.53 for the blue curve. The new samples can be considered as made of independent variables and sharing the same law.

In Fig. 7, the vertical steps of the blue curve are equal to $1/p$ and the vertical distance to the black curve should be of order $1/\sqrt{p}$. A Ugly Duckling in the sampling results in a single large distance $D_\alpha$, inducing a large horizontal step of height still $1/p$ at the top of figure, but such a step has no significant effect on this KS test. One can detect these inconsistencies by testing the maximum $c$ of the $D_\alpha$ using

$$P(\max_\alpha D_\alpha > c) = 1 - P(D < c)^k$$

where $k$ is the number of samples. In our case we get $c = 2.65$ (resp. 1.43) and $P = 6\,10^{-5}$ (resp. 0.26).

Thus the data providing the red curve of Fig. 7 is rejected with both tests.

## V. EFFICIENCY OF VMC

The efficiency of the VMC may be defined as the accuracy obtained with a given CPU time. The standard deviation of the results is given by $\sigma_{\text{eff}}/\sqrt{N}$ where $N$ is the number of retained energies. The CPU time is proportional to the number of steps $M = NE(n) = N/\mathsf{R}_a$. Thus the efficiency of the VMC may be measured with the dimensionless parameter

$$\mathrm{Q} = \frac{\sigma\sqrt{\mathsf{R}_a}}{\sigma_{\text{eff}}} \tag{54}$$

where $\sigma$ is the standard deviation given by the distribution of the energy; i.e. the standard deviation of the VMC for $M$ trials rewrites:

$$\frac{\sigma_{\text{eff}}}{\sqrt{N}} = \frac{\sigma}{\mathrm{Q}\sqrt{M}}. \tag{55}$$

Notice that $\sigma$ is a lower bound for $\sigma_{\text{eff}}$, therefore $\mathrm{Q} \leq 1$.

### A. Experimental results

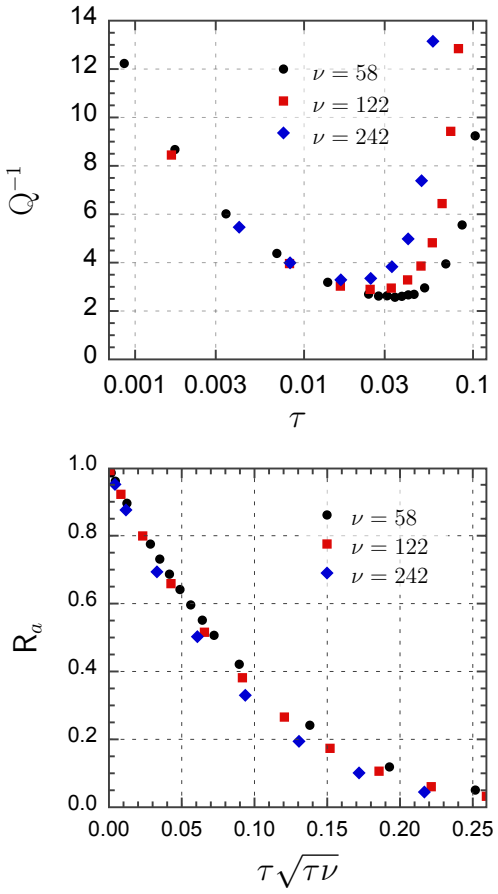


FIG. 8. Inverse efficiency, $Q^{-1}$, and acceptance probability, $R_a$, for different values of the Monte Carlo diffusion time step, $\tau$, and the dimension of configuration space, $\nu$.

Fig. 8 gives the behavior of Q (resp. $R_a$) as a function of $\tau$ (resp. $\tau\sqrt{\tau\nu}$), the time step of the discretized diffusion process. We see that for small $\tau$, Q is a function of $\tau$ only ($\tau$ is normalized in the sense that by Eq. (7) the mean distance between particles does not depend on $\nu$). The behavior of $R_a$ as a function of $\tau\sqrt{\tau\nu}$ is more questionable since the range of $\nu$ is rather limited. Nevertheless, as $\nu$ increases, smaller $\tau$ must be chosen to obtain similar behavior. The behavior of Q for intermediate values of $\tau$ (Fig.8) enforces this relationship between VMC and $\nu$. As it is usually claimed the minimal Q is for $R_a \approx 0.5$.

The scaling law of $R_a$ may be understood as follows. As $\tau$ goes to zero, we have at the leading order:

$$A(R', R) = \min\left(1, e^{\frac{\tau}{2}\left(G(R)^2 - G(R')^2\right)}\right) \tag{56}$$

Let $H$ be the gradient of $G$ (i.e. the Hessian of $\frac{1}{2}\ln P$) then

$$G(R)^2 - G(R')^2 \approx 2(R - R') \cdot HG. \tag{57}$$

Now $R - R' \approx \sqrt{\tau}\eta_\nu$ where $\eta_\nu$ is a vector of $\nu$ normalized Gaussian variables, thus:

$$A(R', R) \approx \min\left(1, e^{\tau\sqrt{\tau}\|HG\|\eta}\right). \tag{58}$$

where $\eta$ is a normalized Gaussian variable. Therefore the acceptance at $R$ is

$$R_a(R) \approx 1 - \frac{\tau\sqrt{\tau}}{\sqrt{2\pi}}\|HG\|. \tag{59}$$

Assuming that $H$ is bounded, we have $\|HG\|^2 \propto \nu$ and

$$R_a \approx 1 - \frac{\tau\sqrt{\tau\nu}}{\sqrt{2\pi}}c \tag{60}$$

Be aware that $c$ in Eq. (60) depends on $P$ and thus on $\nu$ (it is not simple to build equivalent models with different $\nu$). Figure 8 is built from different wave functions, $\Psi$, representing the electron gas at different number of particles but at the same density.

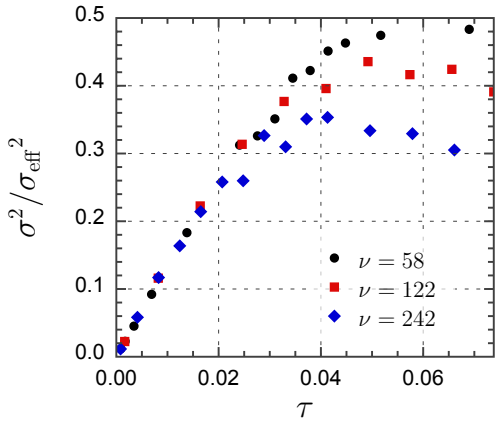


FIG. 9. $\sigma^2/\sigma^2_{\text{eff}}$ as a function of the time discretization. Different patterns correspond to different values of $\nu$ ($\sigma^2 = 0.04, 0.02, 0.01$).

Figure 9 reveals the linear behavior of $\sigma^2/\sigma^2_{\text{eff}}$ for small values of $\tau$. Indeed, as $\tau$ goes to zero, we expect that the the discrete process converges to the continuous process, Eq. (3); in particular $k$ steps at time discretization $\tau$ are equivalent to one step at time discretization $k\tau$. Thus the correlation length scales as $1/\tau$ and $\sigma^2_{\text{eff}}/C_0$ behaves like $1/\tau$. At the same time, $C_0$ goes to $\sigma^2$ the variance of energy since $E(n) = 1/R_a$ goes to 1. Therefore for small $\tau$:

$$Q^{-1} \approx \frac{\sigma_{\text{eff}}}{\sigma} \propto \frac{1}{\sqrt{\tau}} \tag{61}$$

On the other hand, as $R_a$ goes to zero the trials become independent; thus $\sigma^2_{\text{eff}}$ goes to $C_0$ and Eq. (33) gives

$$C_0 \longrightarrow \frac{1}{E(n)(\sum_i n_i)} \sum_i n_i^2 \tilde{X}_i \propto \sigma^2 \tag{62}$$

Thus for small $\mathsf{R}_a$:

$$\mathrm{Q}^{-1} \approx \frac{\sigma_{\rm eff}}{\sigma\sqrt{\mathsf{R}_a}} \propto \frac{1}{\sqrt{\mathsf{R}_a}} \tag{63}$$

### B. Implementaion details

In practice, a raw implementation of QMC leads to blocking configurations as soon as $\tau$ is not very small. Indeed, the probability $P(R)$ comes from an antisymmetric wave function and thus vanishes at least at $r_i = r_j$. If $P(R)$ vanishes then $G(R)$ diverges and this results in very large values of $n_i$. As $\tau$ increases, $|R-R'|$ increases and the nature of the process changes: Eq. (56) is a second order approximation which may be no more relevant. In Eq.10, the factor $\frac{T(R|R')}{T(R'|R)}$ may be very small. Setting $\eta = R' - R - \tau G(R)$, we have:

$$\begin{aligned}\frac{T(R|R')}{T(R'|R)} &= \exp\left(\frac{1}{2\tau}\eta^2 - \frac{1}{2\tau}(\eta+\tau G(R)+\tau G(R'))^2\right)\\ &= \exp\left(-\eta(G(R)+G(R')) - \frac{\tau}{2}(G(R)+G(R'))^2\right)\end{aligned} \tag{64}$$

Here, $\eta$ is a vector of $\nu$ Gausssian variables of variance $\tau$, so $\eta G(R)$ is a Gaussian variable of variance $\tau G(R)^2$. Therefore, if $G(R)^2$ is large, the exponent in Eq. (64) is of order $-\tau G(R)^2$, and, in our simulations, we have to ensure that drift $\tau G(R)$ is bounded, otherwise the exponent may be very large leading to blocking situations.

To avoid these situations, we have rescaled $G$ to ensure that $\tau G^2$ is always bounded by $m_G\nu$.

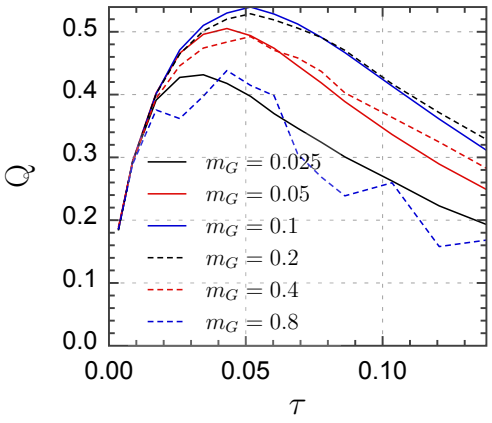


FIG. 10. Efficiency Q as a function of $\tau$ for for different values of $m_G$ ($\nu = 58$ and $r_s = 1$).

From Fig. 10 we see that $m_G \approx 0.05$-$0.4$ gives the best results. For $m_G = 0.8$, the fluctuations of $Q$ becomes important: blocking states occur and the statistics are no more usable.

This has been checked also for $r_s$ (resp. $\nu$) up to 35 (resp. 242). For larger values of $\nu$ the value of $m_G$ is less critical: probably the law of large numbers makes that the relative fluctuations of $G^2$ decrease.

### C. Asymptotic law of $P$

For 20000 trials, $P = |\Psi|^2$ has been found in a range 1-$10^{13}$. This may seem surprising; in fact, this behavior is banal and appears in standard models in statistical physics. As an example, let us consider the momentum distribution of the ideal gas:

$$P(p_1,\dots,p_\nu)d^\nu p = \frac{e^{-\frac{\sum_i p_i^2}{2}}}{\sqrt{2\pi}^\nu} d^\nu p \tag{65}$$

then setting $\phi = \sum_i p_i^2/\nu$, the image (or push-forward) measure of $d^\nu p$ is $V(\phi)d\phi$ where $V(\phi) \propto \phi^{\frac{\nu-2}{2}}$. Thus the the image measure of $Pd^\nu p$ is proportional to:

$$\rho(\phi)d\phi = \phi^{\frac{\nu-2}{2}} e^{-\frac{\nu\phi}{2}} d\phi \tag{66}$$

Then as $\nu$ goes to $\infty$, with probability one $\phi$ is the maximum $\phi_0$ of $\ln(\phi) - \phi$, i.e. $\phi_0 = 1$, and around $\phi_0$

$$\rho(\phi)d\phi \approx \exp\left(-\nu\frac{(\phi-\phi_0)^2}{4}\right) d\phi \tag{67}$$

That is $\phi$ has fluctuations of order $1/\sqrt{\nu}$ and while $\rho(\phi)$ is almost constant, $V(\phi)$ and $e^{-\frac{\nu\phi}{2}}$ have large fluctuations of order $e^{\pm C\sqrt{\nu}}$.

In our case, $\Psi$ is not normalized, thus the mean of $\ln|\Psi|^2$ (proportional to $\nu$) does not make sense but the Gaussian law is clear with a standard deviation $\sigma/\sqrt{\nu} = 0.52$ (Fig.11).

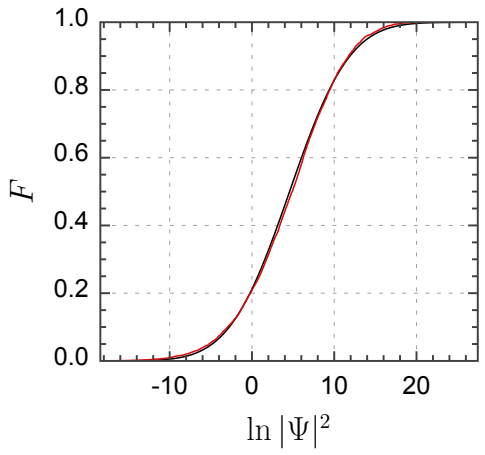


FIG. 11. Repartition function of $\ln|\Psi|^2$ ($\nu = 122$ and $r_s = 10$). Black line is the normal law; red line is obtained with 20000 trials.

The variance of $\ln|\Psi|^2$ should depend on the choice of $\Psi$ but the Gaussian law is expected in any case for large $\nu$; indeed, the Jastrow part of $\Psi$ is usually a product of $\nu^2$ factors and the Slater part is a determinant which is also, in the thermodynamics limit, the exponential of some extensive quantity.

## VI. CONCLUSION

In this paper, we have reviewed well known results of statistics applied to Monte Carlo calculations. We have provided effective algorithms to compute the accuracy and to check the equilibration of Monte Carlo simulations. In order to optimize and understand the limitations of standard variational Monte Carlo sampling, we have further described general scaling laws of the discrete time approximation of the diffusion process with examples on the homogeneous two dimensional electron gas.


[1] K. Binder, *Applications of Monte Carlo methods to statistical physics*,, Rep. Prog. Phys. **60** (1997) 487-559

[2] W. K. Hastings, *Monte Carlo sampling methods using Markov chains and their applications*, Biometrika (1970), **57**, 1, p. 97

[3] R. E. Caflish, *Monte Carlo and quasi-Monte Carlo methods*, Acta Numerica (1998), **7**, 1-49

[4] H. Kalos, P. Whitlock, *Monte Carlo Methods*, 2nd Edition, WILEY-VCH Verlag GmbH & Co, 2008 ISBN 978-3-527-40760-6

[5] G. F. Giuliani and G. Vignale, *Quantum Theory of the Electron Liquid*, Cambridge University Press, Cambridge (2005).

[6] L. Breiman, *Probability*, Addison-Wesley Publishing Company, 1968 ISBN 0-201-00646-4

[7] A. Kolmogorov, *Über die analytischen Methoden in der Wahrscheinlichkeitsrechnung* (On Analytical Methods in the Theory of Probability), 1931 Mathematische Annalen **104** 415-458

[8] Metropolis, N., Rosenbluth, A.W., Rosenbluth, M.N. et al. (1953) *Equations of state calculations by fast computing machines.*, Journal of Chemical Physics, **21**, 1087.

[9] C. Kipnis, S. R. S. Varadhan (1986) *Central limit theorem for additive functionals of reversible Markov process and applications to simple exclusions* Comm. Math. Phys. **104** 1-9

[10] C. J. Geyer, (1992). *Practical Markov chain Monte Carlo*, Statistical Science, 7:473-511.

[11] P. Billingsley, (1995), *Probability and Measure* (third ed.), John Wiley & sons, ISBN 0-471-00710-2

[12] G. Jones, (2004) *On the Markov chain central limit theorem*, Probability Surveys, **1** 299-320

[13] D. Knuth, *The Art of Computer Programming*, vol. 2, third ed., Addison-Wesley Professional, ISBN 0-201-89684-2